FLOW FIELD INVESTIGATION FOR A SERIES OF RIGHT ANGLE MINIMUM AXIAL DEPTH PUMP INTAKES

by

Joseph H. G. Howard

Professor of Mechanical Engineering

University of Waterloo

Waterloo, Ontario, Canada

and

Paul Hermann

Chief, Turbomachinery Research Engineering

Sundstrand Aviation Operations

Rockford, Illinois

Joseph H. G. Howard received his undergraduate engineering education at the Royal Military College and Queen's University, Kingston, Ontario, Canada. His graduate studies in the field of turbomachinery were at the University of Birmingham where he received M.Sc. and Ph.D. degrees. He spent four years with Pratt and Whitney (Canada) in Longueuil, Quebec, with the compressor and turbine aerodynamics group.

Since 1964, Dr. Howard has been a faculty member in the Department of Mechanical Engineering at the University of Waterloo, Ontario, Canada, with the rank of Professor since 1971. His research has included both experimental and analytical investigations of fluid flow in centrifugal compressors and pumps. Dr. Howard has spent short sabbatical leaves with Creare, Inc., in Hanover, New Hampshire, and Sundstrand Corporation, in Rockford, Illinois.

Paul Hermann is Chief of Turbomachinery Research Engineering for Sundstrand Aviation Operations in Rockford, Illinois. He heads a group of engineering specialists engaged in the aerodynamic and hydrodynamic design of turbines, fans, compressors, pumps, and hydraulic torque converters used in Sundstrand turbomachinery. He has 30 years of experience in the design of turbomachinery components and systems, as well as in the design of gas turbines.

Mr. Hermann received his Dipl. Ing. in Mechanical Engineering in West Germany and an M.S. in the U.S.A. He also obtained a diploma in Applied Fluid Dynamics from Belgium.

Mr. Hermann is a member of ASME, VDI and Pi Tau Sigma. He is a registered professional engineer in the State of Pennsylvania.

ABSTRACT

A series of right-angle pump intakes, incorporating minimum axial depths and decelerating flows, has been experimentally evaluated using an air flow test procedure. Performance was measured, internal flow fields observed and a wall streamline flow visualization method was employed with an extension to allow its use on curved surfaces. Diffusing intakes, which are sometimes required in applications such as aircraft fuel pumps, are shown to be sensitive to small changes in internal geometry. The flow structures associated with the observed loss regions are described, together with some implications for intake design.

INTRODUCTION

For some applications, the designer of a centrifugal pump is faced with the necessity of including a right-angle intake with a minimum axial depth. This is often the case for the aircraft fuel pump where, in addition, the use of an axial inducer requires a low flow coefficient at the pump entry, so that two-phase flow and cavitation may be dealt with optimally. This usually results in a large deceleration in the flow from the pump suction pipe to the inducer entry plane. The axial depth limitation arises from both space and weight restrictions.

Ideally, an intake should deliver the fluid to a pump with a minimum loss of total pressure and with uniformly distributed flow. In standard pump practice, this can be achieved by locating any required elbows well upstream of the pump entry. Alternatively, right-angle intakes may be incorporated in the design of pump casings where side-suction or double-suction pumps are involved. A brief review of such intake shapes and their associated losses was made by Kovats [1]. From those data it may be observed that a common feature of the better inlet shapes is a reducing cross-sectional area, hence accelerating flow. The axial depths are also greater than aircraft fuel pump practice would frequently allow. A detailed study of the redesign of a pump side intake was described by Pilarczyk and Rusak [2]. The study was based on an air flow model, and surface flow visualization was employed, using oil and lampblack to produce wall streamline traces. Velocities were measured with a traversing four-hole pressure probe. In a study on side inlet box geometries for axial fans, Bernard [3] tested only shapes producing accelerating flow. Even with a strongly accelerating flow in the inlet box, the fan efficiency was sensitive to adjustments to the shape of the inlet box.

Since little organized data was available on right-angle intakes which incorporated the combination of flow diffusion

and reduced axial depth found in many aircraft fuel pump applications, an experimental program was undertaken to measure the flow field and losses in such geometries. An air flow model was employed and observations or measurements were made of total pressures, wall static pressures, flow angles and wall streamline directions. The test series included two families of geometries and variations within those geometries. The intention was to set up a testing procedure simple enough to allow the study of many geometric variations, while complete enough to provide worthwhile comparisons between intakes and to describe the major features of the flow field in such geometry. The performance was evaluated by the measurement of total pressures at the pump entry plane where wall static pressures and flow angles were also observed. The flow pattern was studied through the observation of wool tuft action and the use of a special wall-streamline flow visualization method. The important question of the interaction of the distorted flow in the intake with the flow field in the pump rotor could not be addressed in this study.

The experimental methods, the basic geometric features of the intakes under study and the results of the performance and flow visualization observations are described. A discussion is included on the probable links between the intake geometry and the observed flow field and on the implications of this study for intake design procedures.

EXPERIMENTAL APPARATUS

The arrangement of the test rig is shown in Figure 1. Air was drawn through the test section and the drum-shaped plenum chamber by a radial-bladed centrifugal fan, driven by a 50 hp motor. The flow was controlled by a blast gate located upstream of the fan in the 12 in diameter pipe which linked the plenum and fan. A clear plastic pipe of 7.68 in diameter, emerging at the center of one of the faces of the plenum, simulated the shroud of an inducer section of a pump. The inducer hub was simulated by a cone mounted on the opposite plenum wall. It carried instrumentation and was rotatable.

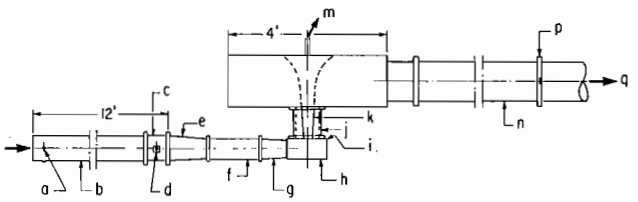

Figure 1. Experimental Rig—Plan View, Showing (a) Inlet Static Pressure Taps (4) to Measure Flowrate; (b) Calibrated Entry Pipe (7¾ in Diameter); (c) Calibration Traverse Section; (d) Traverse Location; (e) Transition Cone; (f) Straight Pipe, Intake Entry Diameter, Three Diameters Long; (g) Intake (Section from Entry to Doughnut); (h) Doughnut Portion of Intake; (i) Pump (Inducer) Entry Plane; (j) Clear Plastic Tube (Shroud); (k) Conical Hub Section—Rotatable with Probes; (m) Tubes from Probes Emerge at Rear of Drum-Shaped Plenum; (n) Outlet Pipe (12 in Diameter); (p) Blast Gate Flow Control; (q) to Fan.

A straight pipe of 12 ft length and 7¾ in inside diameter served to carry air from the room to the tested intake or directly to the pump entry plane. A sharp-edged entry provided a stable flow, while a convenient static pressure measurement near the vena contracta was used to determine the flowrate. The flow calibration was established by Pitot-tube traverses across the straight pipe near the plenum. The total pressure loss associated with the flow entry into the straight pipe was measured at the simulated pump entry plane by attaching the straight collector pipe directly at that plane without using a model intake. This value was subtracted from the measured head loss for each intake in calculating the intake total pressure loss coefficient K.

Since intakes had different entry diameters, transition pieces had to be provided consisting of a conical section with 16° total cone angle and a straight pipe of three diameters in length.

The flowrate was adjusted for each entry geometry to maintain the Reynolds number constant, based on the flow at the pump annulus entry plane. The corrected Reynolds number for the tests was 2.74×10^5 ($\pm 0.06 \times 10^5$).

GEOMETRY OF TESTED INTAKES

For purposes of discussion and analysis, each intake may be divided into two parts. The portion in which the flow turns 90° and enters the pump annulus is termed the "doughnut." The portion which carried the flow from the entry pipe must change its cross-sectional shape from circular to a shape which suits the doughnut, usually nearly rectangular, and may have diffusion and/or curvature.

Two families of intake geometry were tested and are described here under the labels A and B. The intake geometries are summarized in Table 1. All had an inducer (pump entry) shroud diameter of 7.68 in and inducer hub diameter of 2.69 in, but differed in entry pipe diameter and axial depth. The area ratios, A_1/A_2, A_2/A_3 and A_1/A_3, indicate the average flow diffusion in the entry portion, the doughnut portion and the overall intake. The dimensions shown are those of the internal flow passages.

Series A Intakes

Intakes A-1 to A-4 used a common doughnut, shown in Figure 2, which was manufactured from clear plastic for ease of flow observation. The intake A-3 utilized the same doughnut, with a spacer added to increase its axial depth. Some tests were carried out with modifications to the doughnut, also illustrated in Figure 2. The "basic doughnut" had no obstructions except for the central cylinder simulating the pump shaft and the blade (flow divider) situated opposite the flow entry. On some varia-

Table 1. Summary Comparison of Intake Geometries (Dimensions in inches). A_1—area at entrance of intake section. A_2—area at entrance of bellmouth. A_3—area at pump entry plane (annulus).

Intake	(Transition Piece) Entry Pipe Dia.	Axial Intake Depth	Area Ratios		
			A_1/A_2	A_2/A_3	A_1/A_3
A-1	5.18	3.78	0.66	0.79	0.52
A-2	6.40	3.78	1.0	0.79	0.79
A-3	7.75	5.42	1.02	1.14	1.16
A-4	5.18	3.78	0.66	0.79	0.52
B-1	6.40	3.18	0.66	1.20	0.79
B-2	7.75	3.00	1.0	1.16	1.16

tions, the blade was moved around the periphery by +30° (counterclockwise) or −30° (clockwise). In another variation, the doughnut cavity, which extended outward beyond the inducer shroud diameter, was filled on the side opposite the entry, as shown in Figure 2. Still another variation involved the insertion of posts within the flow passages. These posts, shown extending axially across the flow passages in Figure 2, could be sometimes desired in a pump for structural reasons.

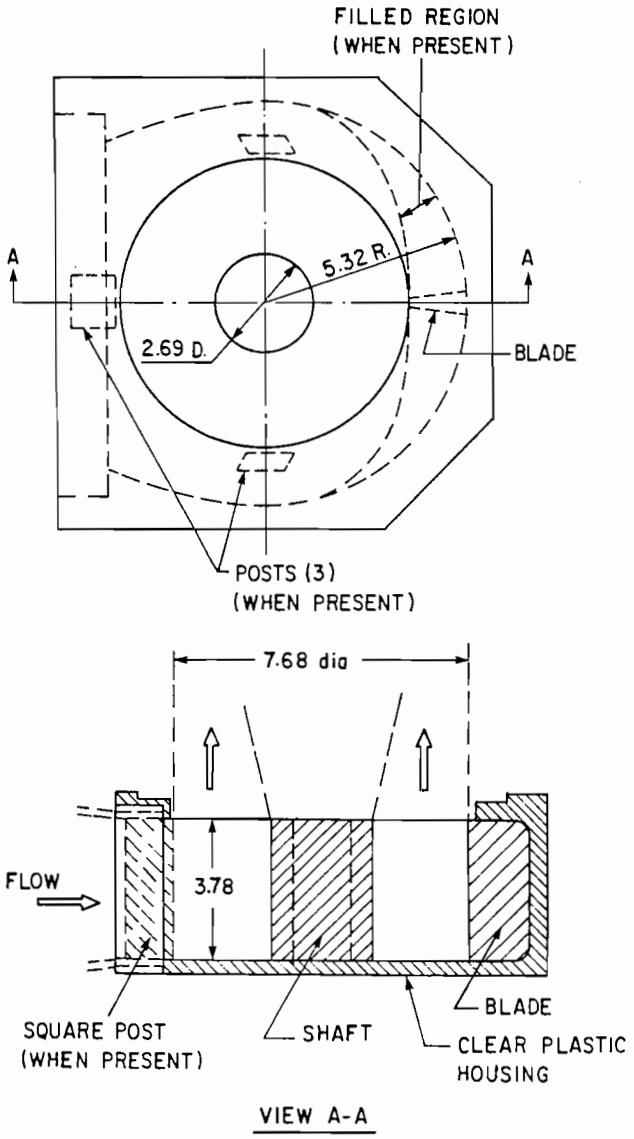

Figure 2. Clear Plastic Doughnut for Series A Intakes. The A-3 intake used the same doughnut with axial depth increased to 5.42 in. (All dimensions in inches.)

The shape of the entry portions of intakes A-1, A-2, A-3 and A-4 are illustrated in Figure 3. The contour shown is that of the inside of each intake portion, which was manufactured of fiberglass formed over a wood and plaster mold. Intakes A-2 and A-3 had no diffusion in this portion, but A-1 and A-4 had the area ratio A_1/A_2 of 0.66, with the A-4 intake incorporating a long-radius 90° bend.

The assembly of the A-1 intake with the plastic doughnut mounted on the rig is shown in Figure 4. The transition piece is shown here, but the three-diameter long straight pipe between the transition piece and intake is missing from this view, although it was included for all reported performance tests.

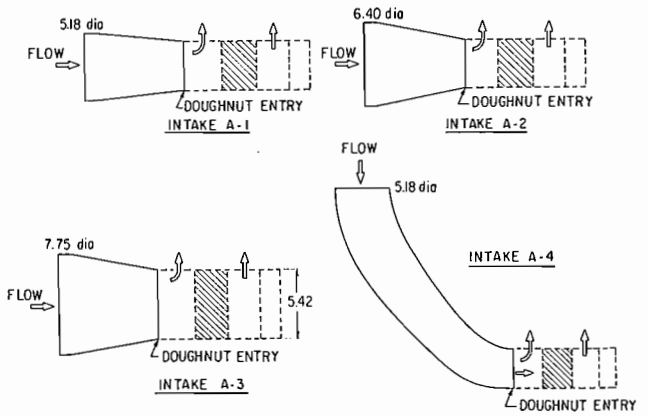

Figure 3. Entry Portions of Intakes A-1 to A-4. (All dimensions in inches.) See Table 1 for other dimensions.

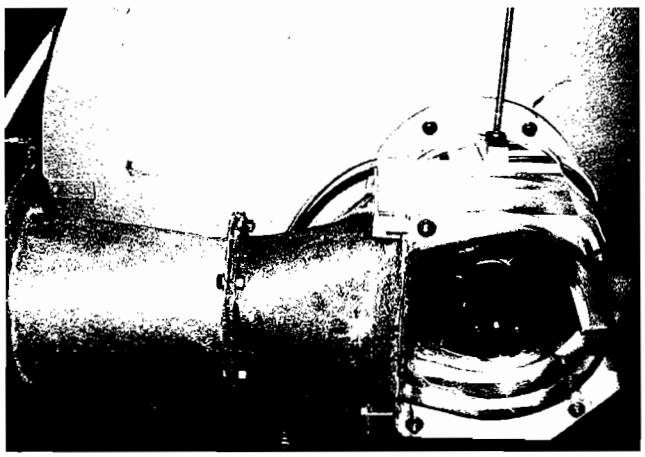

Figure 4. View of Intake A-1 Mounted on Test Rig. During tests, a straight pipe of three diameters in length was inserted between the transition cone (at left) and the intake.

Intake Series B

This intake was designed to incorporate a very short axial depth and a constant velocity or accelerating turn from radial to axial flow in the doughnut. Thus, it included a bellmouth shape extending from the inducer shroud and a very broad skirt around the central shaft. Intake B-1, shown in Figure 5, had the same overall area ratio as intake A-2 and was tested with and without vanes in the diffusing section of the intake between the entry pipe and the doughnut. Intake B-2, whose doughnut cross-section is shown in Figure 6, had the same overall area ratio as intake A-3, thus allowing the study of flow patterns in the series B geometry without a diffusion zone.

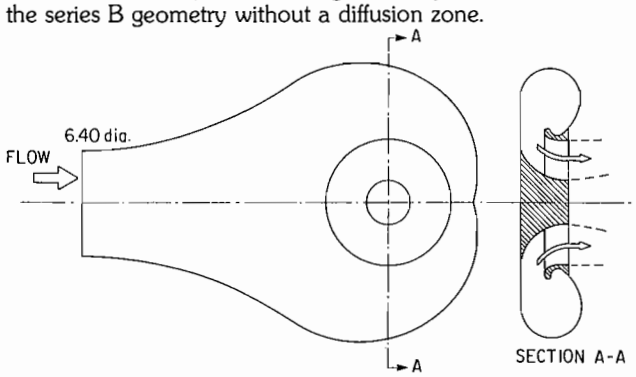

Figure 5. Intake B-1 (All dimensions in inches). See Table 1 for other dimensions.

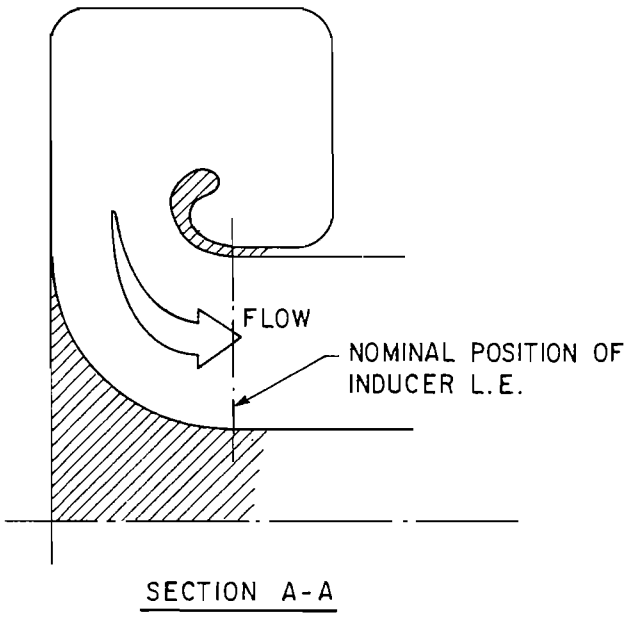

Figure 6. Cross-Section of Intake B-2. Cross-section A-A is positioned in the same way as on Figure 5.

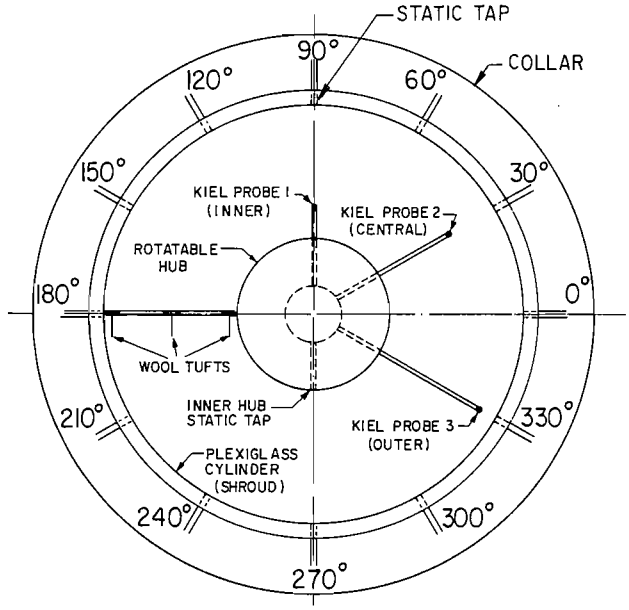

Figure 7. Probe Locations and Definition of Angular Coordinate at the Pump (Inducer) Entry Plane (Flow enters intake from left).

EXPERIMENTAL TECHNIQUES

Measurements at the Pump Entry Plane

At the pump entry plane, total pressure measurements were obtained by mounting three Kiel probes, so that they extended from the hub to the radii determined by the centers of three equal-area annuli. The tubes from these probes, and the tube from a wall static tap also mounted on the hub, extended to the rear of the plenum through the hollow center of the rotatable hub. Shroud wall static taps were located at 30° intervals around the clear plastic tube on the same plane. The locations of all of this pressure measurement instrumentation are shown in Figure 7. This figure also defines the angular location coordinate θ. For all intakes, the flow enters the doughnut from the region near $\theta = 180°$, while $\theta = 0°$ is positioned at the usual location of the flow divider (blade). The hub was rotated in 30° intervals, and the pressure was measured with a pressure transducer connected to each of the lines through a scanning valve assembly.

The total pressure loss, at any measurement location, which can be attributed to an intake is the total pressure measured by the Kiel probe, below atmosphere, less the same measurement taken with the straight pipe attached directly to the pump entry plane without an intake section. This was used, after dividing by the velocity head at that plane, to determine the total pressure loss coefficient K reported herein. The total pressure loss measured in this way included losses through the transition cone and subsequent short pipe. These transition sections are used with intakes A-1, A-2, A-4 and B-1. To obtain an adjusted average total pressure loss coefficient (K adjusted-presented only in Table 2) the loss through the transition cone and pipe was calculated, using published coefficients [4].

Wall static pressure measurements at the pump entry plane were intended to enable velocity calculations using the assumption of a linear static pressure variation with radius from the hub to the shroud. This procedure proved unreliable, in the presence of flow distortions, and no observations are reported here.

The flow angle at the pump entry plane was approximately determined by the observation of wool tufts positioned at three radial locations on a rod mounted on the hub, as shown in Figure 7. The tufts were held to the rod by a wire ring attached to the tuft and positioned by beads on the rod. The recorded angle components were the component in the meridional plane, ϕ, positive when outward, and the swirl angle component, λ, positive for clockwise direction, viewed from the intake. For series A intakes, observations could be made both through the intake doughnut and through the inducer shroud. For the series B intakes, only the latter observation direction was possible. A principal purpose of the wool tuft observations was to establish regions of flow oscillation or reversal. The nature of the observation, for one intake, was recorded by a multiflash photographic technique, using eight flashes at 60 Hz.

Observations of Flow Within the Intakes

Within two of the series A intakes, flow angle observations were made using wool tufts on rods extending from the central shaft. The data are not presented here, but served to corroborate conclusions drawn from other evidence.

An important technique employed to study the intake flow patterns was the wall streamline flow visualization method of Langston and Boyle [5]. For the series A intakes, the wall streamline traces were observed on the flat back surface opposite the pump entry plane. The procedure here was virtually identical to that described by Langston and Boyle. A clear plastic sheet was fastened to the flat interior surface. On it, small crosses of permanent marker ink were distributed in a regular pattern using different colors. The plastic sheet was sprayed with oil of wintergreen, with the flat surface maintained in a horizontal position. The intake was quickly put in position on the rig and the fan operated. The marker ink formed streaks which displayed the wall flow direction. Care was required in regulating the amount of oil sprayed on the ink so that suitable streaks would form, while avoiding gravity streaks before the test flow began. Gravity effects during the test were not a problem at the velocities present in the intake.

For the series B intakes, the technique had to be modified to allow it to be applied to curved surfaces. After some trials, it was discovered that a white urethane paint (brand name Varathane) provided a suitable surface for the ink dots and was

not damaged by the oil of wintergreen. After test completion and photographic recording, the ink was easily removed by wiping the surface with oil of wintergreen. Preparatory to the testing procedure, the intakes were cut on a plane normal to the pump axis and arranged for quick reassembly. The procedure was otherwise as described for the series A intakes.

Estimates of Experimental Accuracy

The flowrate calibration, based on flow field traversing, was judged to be repeatable within 2 percent. The Reynolds number variation between tests was within ±2.5 percent. The total pressures sensed by the Kiel probes should be within 0.5 percent of a typical reading, except where the flow angle exceeded 45° from the axial direction. Unfortunately, many regions in some intakes did go outside this criteria. The pressure transducer and display was also judged to be repeatable to one percent. The total pressure drop through the transition cone and associated straight pipe for all intakes except A-3 and B-2 has been accounted for in the adjusted K value in Table 2. This adjustment has not been included in values of K presented elsewhere. The measured angles are believed to be within ±5° for the A series intakes, except where large oscillations or swirling were observed. For the B series intakes the awkward observation angle made the accuracy approximately ±10°.

The average total pressure loss coefficient (K) was based on an area average and included all positions irrespective of the measured flow angle. Mass flow averaging was not feasible, due to the unreliable velocity values. Test repetition, involving a complete disassembly and reassembly of test components, indicated repeatability of K (average) within ±0.07. Average K values for the more efficient intakes could be somewhat low, since the Kiel probe locations would not have responded to losses in thin boundary layer regions.

MEASURED PERFORMANCES AND OBSERVED FLOW FIELD

Total Pressure Loss

The measured values of total pressure are presented in terms of a total pressure loss coefficient K on Figures 8 to 12, for each combination of geometry. The coefficient K is defined as

$$K = \frac{\Delta p_{tot}(\text{intake}) - \Delta p_{tot}(\text{straight pipe})}{\frac{1}{2}\rho V_3^2}$$

where V_3 and ρ are the average velocity and density at the pump inlet plane, respectively. The average K is a simple area average resulting from the averaging of all local values. This is presented in Table 2 along with an adjusted average K which accounts for losses in the transition cone and pipe based on published data [4]. Loss prediction for a contraction cone was combined with the smooth pipe loss (L/D = 3) for fully developed flow.

Also shown in Table 2 is one measure of the flow distortion, the maximum difference of K recorded at the measurement points for an intake, labelled K(max-min). In general, this distortion measure varied in step with the average K value.

Loss in Series A Intakes

An examination of Figures 8 to 11 shows two principal loss locations. The most extensive region of high loss is located near θ = 180°, usually extending from 120° to 240° for the outer Kiel probe. This loss is associated with a separation zone, as the flow turns the sharp corner from the radial to the axial direction. The zone is illustrated in Figure 13, which also shows a twin vortex formation, which developed to each side of the flow divider. The associated loss peaks are clearly seen for intake A-1 with the basic doughnut (Figure 8). They were situated at 30° and

Table 2. Summary of Average Total Pressure Loss Coefficients.

Intake	Geometry	K(average)	K(av)(adjusted)	K(max-min)
A-1	Basic 0° Blade	2.29	2.06	10.1
	Basic 30° Blade	2.71	2.48	7.5
	Basic −30° Blade	2.31	2.08	7.9
	Posts(3) 0° Blade	2.71	2.48	7.0
	Posts(3) 30° Blade	2.85	2.62	7.1
	Posts(3) −30° Blade	3.03	2.80	7.9
	Filled	8.99	8.76	12.3
	Filled and Posts(3)	3.71	3.48	7.4
A-2	Basic	1.04	0.94	4.9
	Posts(3)	1.70	1.60	6.1
	Filled	2.68	2.58	10.8
	Filled and Posts(3)	1.63	1.53	6.4
A-3	Basic	0.18	0.18	1.1
	2 Posts(90° & 270°)	0.24	0.24	1.2
	3 Posts	0.60	0.60	2.2
A-4	Basic	1.85	1.62	5.2
	Posts(3)	2.26	2.03	5.7
	Filled	2.55	2.32	8.8
	Filled and Posts(3)	2.12	1.89	5.7
B-1	Basic diffuser	1.34	1.24	4.5
	Diffuser with splitters	1.38	1.28	4.2
	Reduced side area	1.36	1.26	4.8
B-2		1.05	1.05	3.8

330° for the middle Kiel probe. Further insight into the nature and formation of these vortices is provided by the flow angle and wall streamline observations.

The geometric variations in intake A-1 modified the loss in one or both of these regions. Moving the blade (flow divider) from its location at $\theta = 0°$, where it served to prevent swirling flow in the intake, to $+30°$ (330°), moved the measured location of the twin vortex loss accordingly. The introduction of three posts into the doughnut (Figure 2) resulted in a mixing out of the twin vortex loss peaks and increased loss for the inner and middle Kiel probes in the $\theta = 120°$ to 240° range. The filling of the doughnut cavity (Figure 2) produced a sharp rise in the loss coefficient, especially for the inner and middle Kiel probes

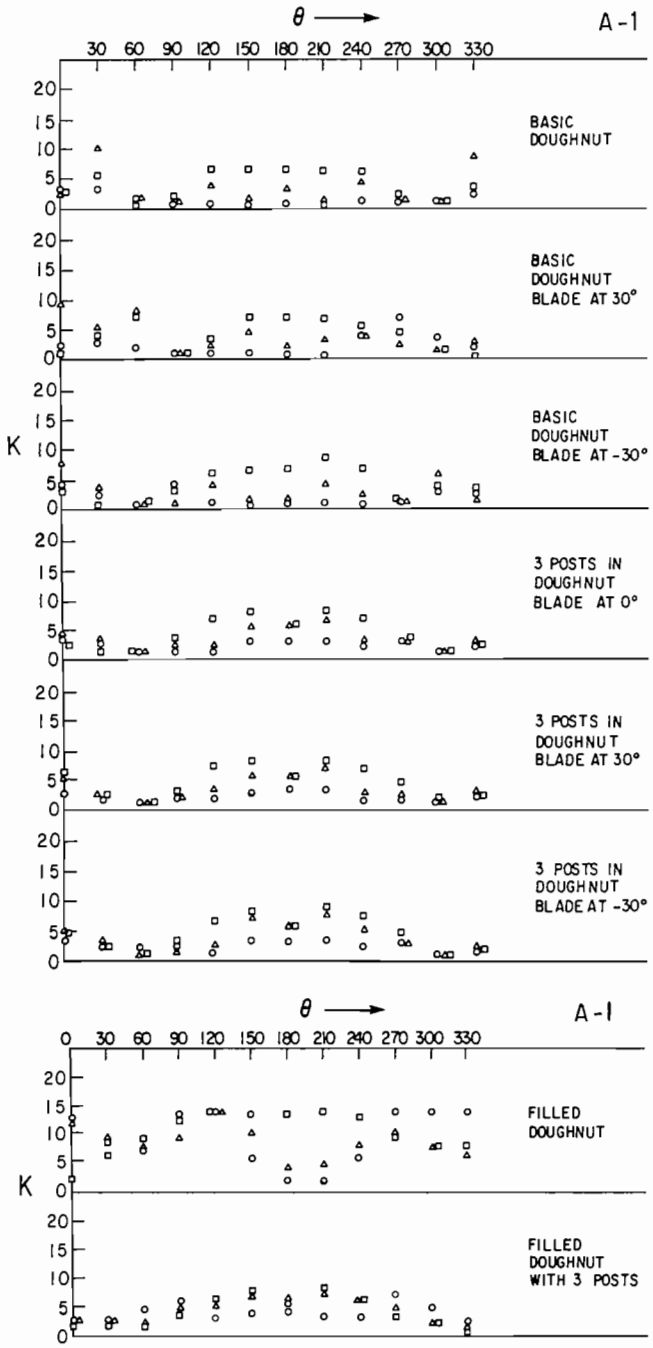

Figure 8. Total Pressure Loss Coefficient K VS Angular Position θ—Intake A-1 (K based on velocity head at pump inlet plant) (o inner probe, Δ middle, □ outer).

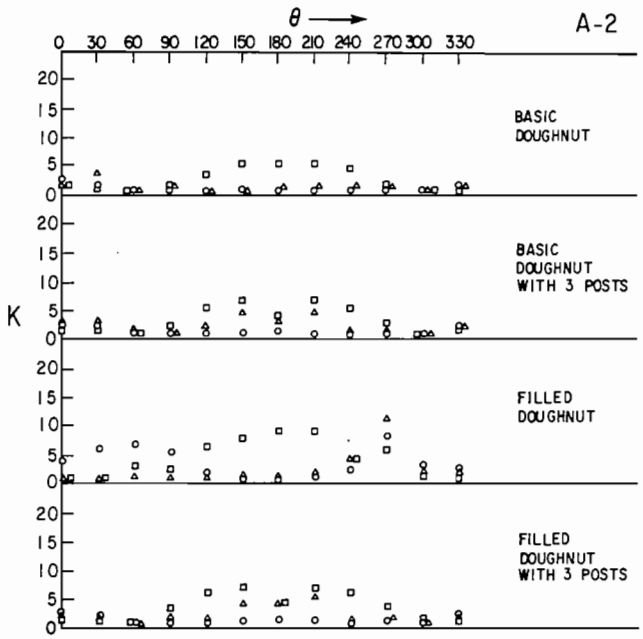

Figure 9. Total Pressure Loss Coefficient K VS Angular Position θ—Intake A-2 (o inner probe, Δ middle, □ outer).

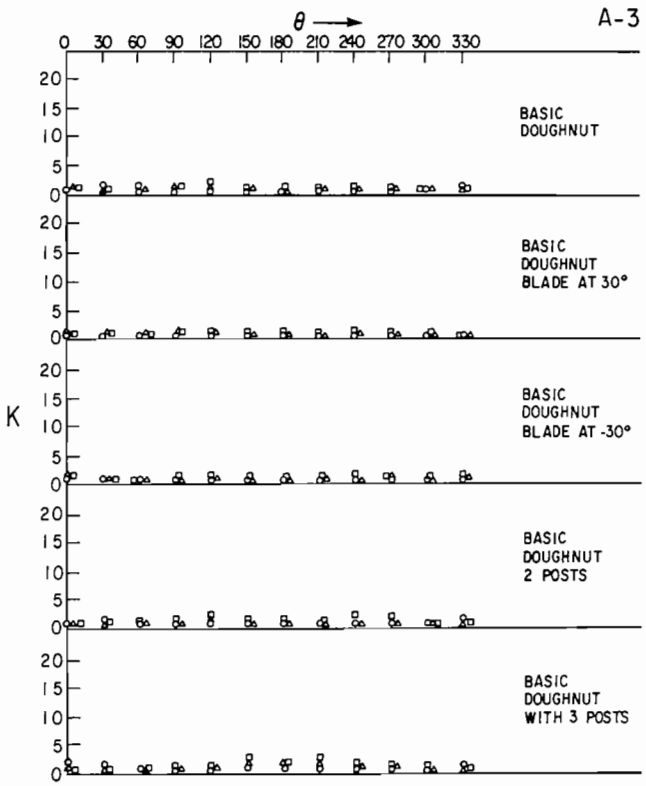

Figure 10. Total Pressure Loss Coefficient K VS Angular Position θ—Intake A-3 (o inner probe, Δ middle, □ outer).

in the region near the twin vortex locations. These losses were sharply reduced when the three posts and filled doughnut were used together.

The intake A-2, as seen in Table 2 and Figure 9, had lower losses than intake A-1, due to the absence of diffusion in the portion of intake directing the flow to the doughnut. This lower loss was most marked in the twin vortex region. The geometry modifications to the doughnut had the same effect as that observed for intake A-1.

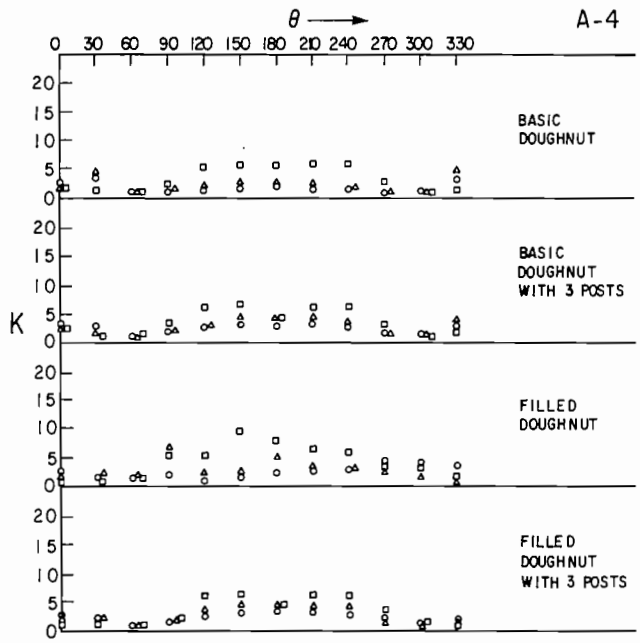

Figure 11. Total Pressure Loss Coefficient K VS Angular Position θ—Intake A-4 (o inner probe, Δ middle, □ outer).

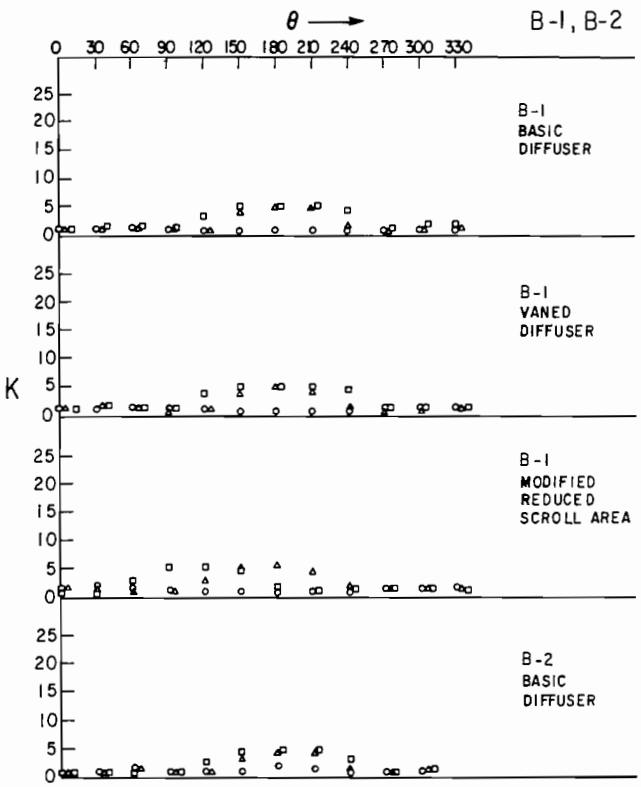

Figure 12. Total Pressure Loss Coefficient K VS Angular Position θ—Intakes B-1 and B-2 (o inner probe, Δ middle, □ outer).

Intake A-3, with a deeper doughnut, had mildly accelerating flow and Table 2 and Figure 10 illustrate the associated lower loss. A separation zone in the θ = 120° to 240° region was still just barely observable. The intake A-4, whose performance is presented in Table 2 and Figure 11, had the same overall diffusion as A-1, but lower losses were observed. Apparently, the long curved diffuser of A-4 delivered more orderly flow to the doughnut than the short diffuser of the A-1 intake.

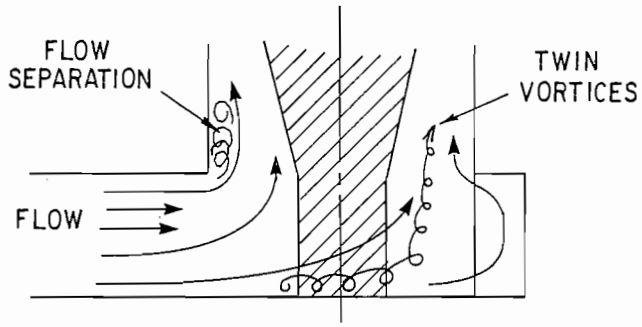

Figure 13. Location of Total Pressure Loss in Series A Intakes—Schematic Diagram.

Loss in Series B Intakes

Despite the more complex shape, intake B-1, with the same overall area ratio as A-2, and intake B-2, with an area ratio matching that of A-3, had higher losses than their equivalents from series A intakes. They did, however, achieve reasonably well distributed flow, with significantly reduced axial depth. The performances are presented in Figure 12 and Table 2. The twin vortex loss peaks did not appear in the B series intakes, but the high loss region from θ = 120° to 240° was still present.

Modifications in intake B-1, by introducing splitter vanes in the diffuser upstream of the doughnut section and by reducing the side areas of the doughnut section, had only minor effects on the performance.

Flow Angle Observation

Sample observations of the wool tuft angles at the pump entry plane are presented in Table 3. Intakes A-1 and B-1 have been chosen as illustrations. The symbol S indicates swirling flow where the tuft spun about its support shaft. LF indicates large fluctuations while OH indicates that the tuft lay along the hub surface and BF denotes back flow. It was observed that the B series intakes had more stable flow at the pump entry plane.

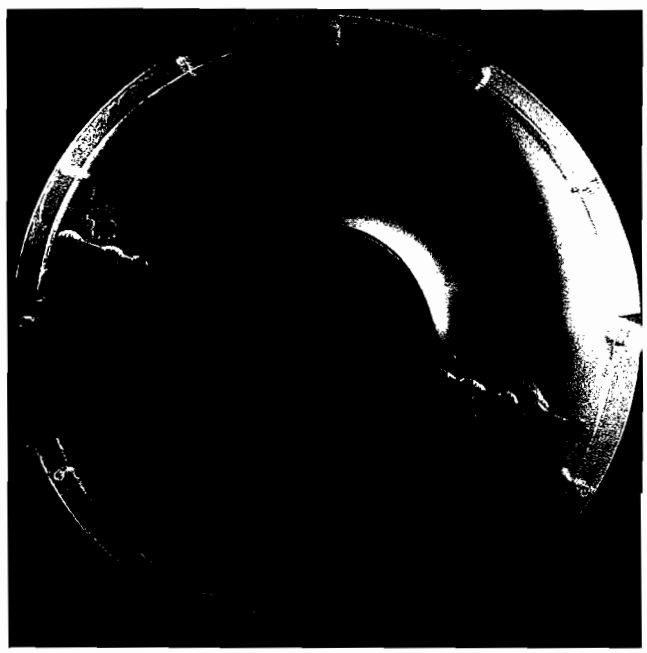

Figure 14. Observation of Wool Tufts at Pump Entry Plane for Intake A-1. Probes at θ = 165° and 345°. Multiflash photo with eight flashes at 60 Hz.

Photographic observations of wool tuft movement at the pump entry plane for intake A-1 are presented in Figures 14 and 15. For these observations, two posts with wool tufts were mounted on the hub, with no Kiel probes. The typical fluctuation in the separated flow region, $\theta = 120°$ to 240°, is shown in Figure 14. The swirl associated with one of the twin vortices ($\theta = 30°$) is shown in Figure 15.

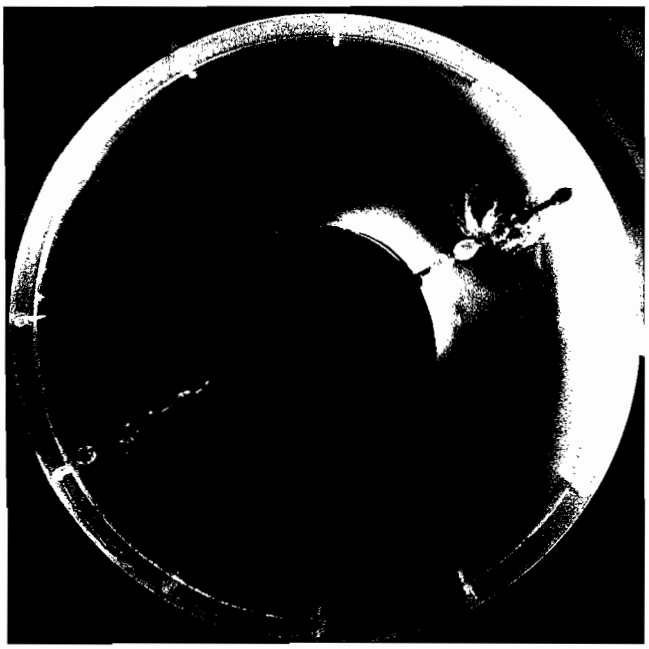

Figure 15. Observation of Wool Tufts at Pump Entry Plane for Intake A-1. Probes at $\theta = 30°$ and 210°. Multiflash photo with eight flashes at 60 Hz.

Wall Streamline Observations

Series A Doughnut

The wall traces in intake A-2 produced on the plastic film by the ink dot method are reflected in Figure 16. The photograph was taken through the reverse side of the plastic film, so that the flow pattern is that seen through the clear plastic wall of the doughnut. The twin vortices are clearly visible. A separation zone is also present just upstream of the shaft. The wall traces produced when intake A-2 was operated with two posts (at 90° and 270°) are presented in Figure 17. The twin vortices are still present on the doughnut wall, although Kiel probe measurements had shown the loss peaks dissipated.

Wall traces on intake A-3, without posts and with posts, are shown in Figures 18 and 19, respectively. Even in this low-loss intake, the twin vortices are visible, although they became less precisely positioned in the presence of the posts.

Series B Intakes

Views of the wall streamline traces on the inner surfaces of the B-1 intake are presented in Figures 20, 21 and 22. The streaks on the intake surfaces show good flow control by the wall, especially for that flow directed toward the hub region. The only significant separation zone was that upstream of the bellmouth lip (Figures 21 and 22). The wall streamlines on the shroud near the pump entry plane showed regions of swirl and reverse flow from $\theta = 120°$ and 240°.

Similar views of the B-2 intake are seen in Figures 23, 24 and 25. The remarkably well-behaved flow is evident in these wall streamline traces, so that the one major problem area stands out. A twin vortex circulation pattern is evident on the shroud wall at the pump entry region (Figures 24 and 25). Some signs of separated flow are also evident in the region where the flow divided to both sides of the doughnut.

Table 3: Wool Tuft Angle Observations. ϕ = angle toward radial; λ = angle toward tangential (+ clockwise) S = swirl; LF = large fluctuations; BF = back flow; OH = on hub.

Intake A-1						
	INNER		CENTRAL		OUTER	
θ	ϕ	λ	ϕ	λ	ϕ	λ
0	OH	±45	−50	±45	−80	±20
30	±10	−30	S	S	S	S
60	OH	±30	20	35	20	30
90	10	40	30	40	LF	±30
120	OH	45	−20	45	−30	±30
150	OH	30	−20	30	−20	20
180	0	0	0	0	S	S
210	OH	±20	−20	−10	−30	−20
240	10	−15	−30	−50	−20	0
270	20	−20	20	−20	LF	±20
300	0	±10	20	−20	LF	−25
330	0	30	S	S	LF	−45
Intake B-1 Vaned Diffuser						
	INNER		CENTRAL		OUTER	
θ	ϕ	λ	ϕ	λ	ϕ	λ
0	0	±10	−10	±10	0, −20	±10
30	0	±10	0	±10	0, −10	±15
60	0	−10	0	10	−20	±15
90	0	0	10	10	−10	15
120	0	±10	0	± 5	0, −15	± 5
150	0	5	± 5	5	S	S
180	0	0	0	0	BF	BF
210	5	0	− 5	0	S	S
240	5	0	5	± 5	±15	±10
270	5	0	5	0	5	0
300	5	5	0	− 5	±10	− 5
330	0	− 5	0	10	0, −20	±15

DISCUSSION

Relationship Between Geometry and Loss

The average total-pressure loss coefficient K_{av}, noted on Table 2, was strongly influenced by the intake area ratio (Table 1). An increase in intake flow diffusion was accompanied by an increase in loss, although geometry changes within an intake could produce even more severe changes in the local coefficient. The K_{av} values measured in the mildly accelerating intakes A-3 and B-2 ($A_1/A_3 = 1.16$) were in the same range as those reported by Kovats [1] for more strongly accelerating shapes, after adjustment for definitions of loss coefficients. Bernard [3] reported the effect of inlets on fan head and efficiency, thus incorporating the interaction of intake and rotor, a factor not included in the present study. His more strongly accelerating intake, with an equivalent A_1/A_3 of 2.34, was markedly better than his intake with A_1/A_3 of 1.63.

Two major loss locations were observed in the A series intakes and one in the B series intakes. The most important loss region was in the $\theta = 120°$ to 240° portion within the outer part

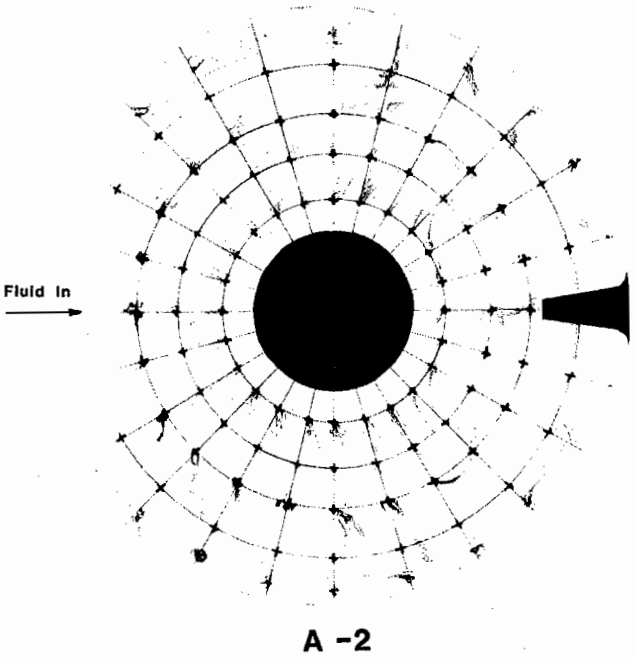

Figure 16. Wall Streamline Traces on Flat Face of Doughnut. Intake A-2 with basic doughnut.

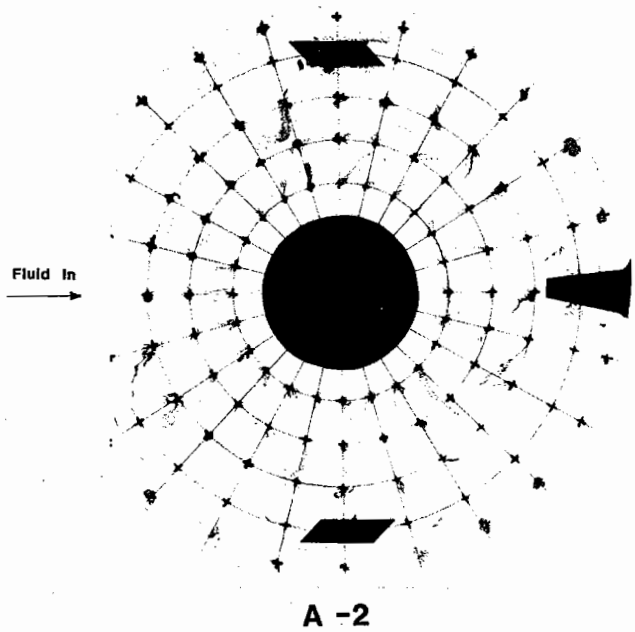

Figure 17. Wall Streamline Traces on Flat Face of Doughnut. Intake A-2 with posts at 90° and 270°.

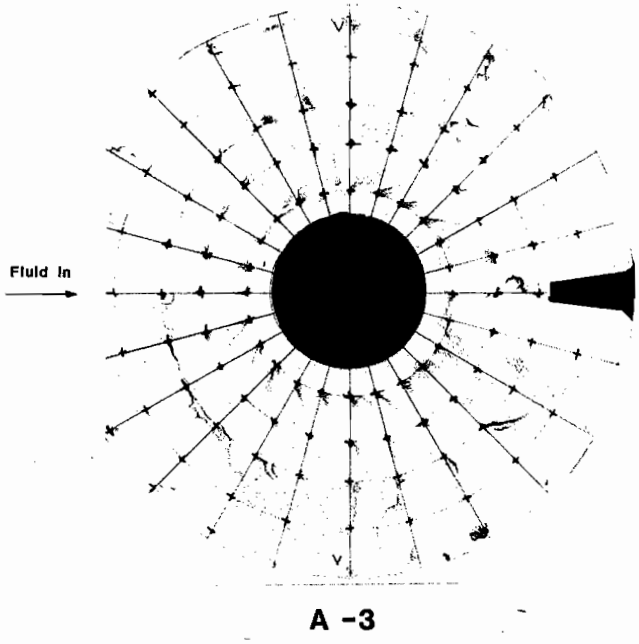

Figure 18. Wall Streamline Traces on Flat Face of Doughnut. Intake A-3 with basic doughnut.

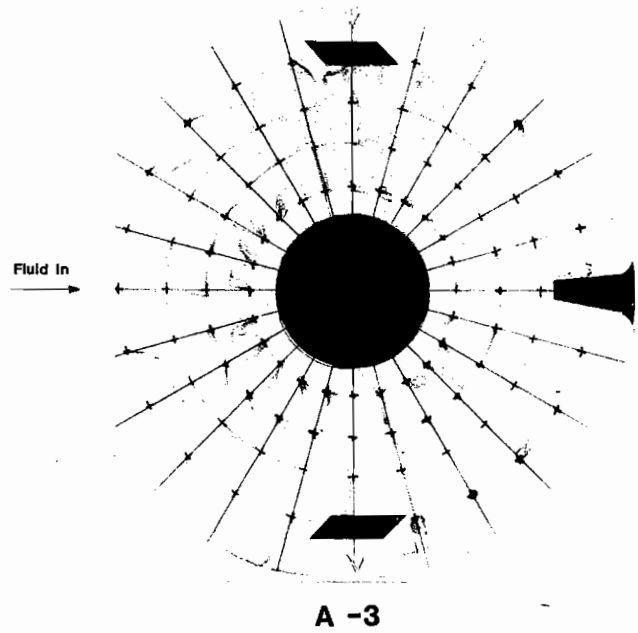

Figure 19. Wall Streamline Traces on Flat Face of Doughnut. Intake A-3 with posts at 90° and 270°.

of the annulus. In the A intakes, this was associated with flow separation at the sharp corner between the doughnut and pump annulus, illustrated in Figure 13. The implication is that more gentle curvature and an increase in axial depth in this region should reduce the losses. However, the evidence from the series B intakes shows that gentle curvature alone did not eliminate this high loss region. In the B series intakes the character of the flow here had changed. Two vortices were present in the annulus, with radial axes, based on the evidence of the wall streamline traces. The flow seemed to be undergoing a three-dimensional separation on the annulus wall as the mainstream flow swung out toward each side channel and then back to enter the annulus in the $\theta = 180°$ region. A cure for this local flow distortion problem is the key to turning the B series intakes into high efficiency designs.

Geometry Influences in Series A Intakes

The second major loss regeneration region in the series A intakes was located near the mid-annulus radius at $\theta = 30°$ and 330° and was associated with the twin vortex flow pattern observed on the flat wall of the doughnut. The twin vortices were formed on each side of the blade (flow divider) and influenced to some extent by the shaft wake and by the

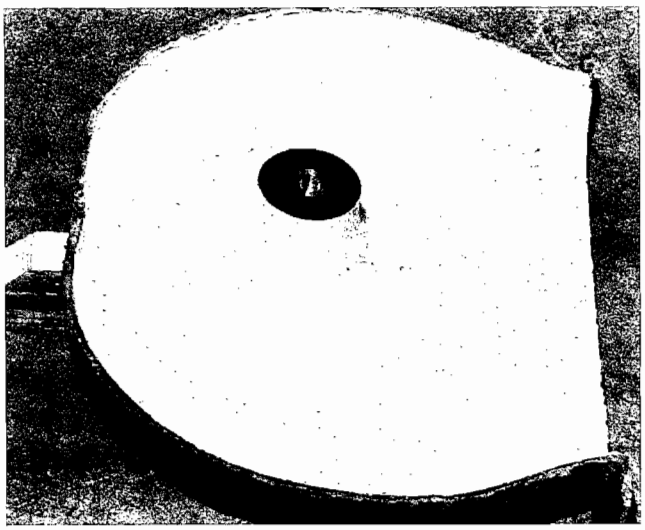

Figure 20. Wall Streamline Traces on Interior of Intake B-1. View of intake half-section opposite pump entry plane. Flow enters from the right.

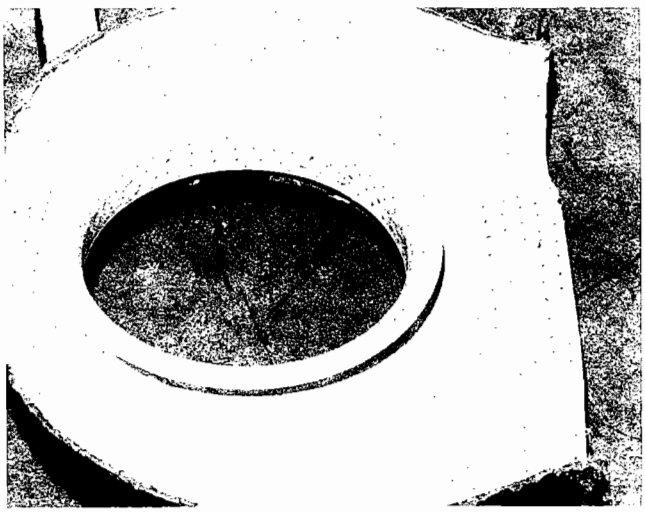

Figure 21. Wall Streamline Traces on Interior of Intake B-1. View of intake half-section including pump entry plane. Flow enters from the right.

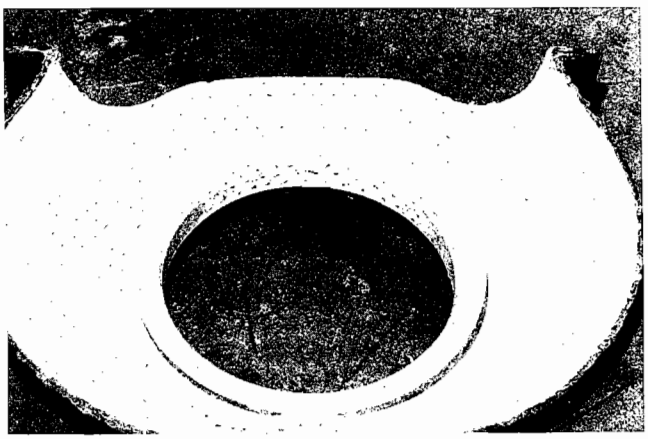

Figure 22. Wall Streamline Traces on Interior of Intake B-1. View of intake half-section including pump entry plane. Flow enters from top.

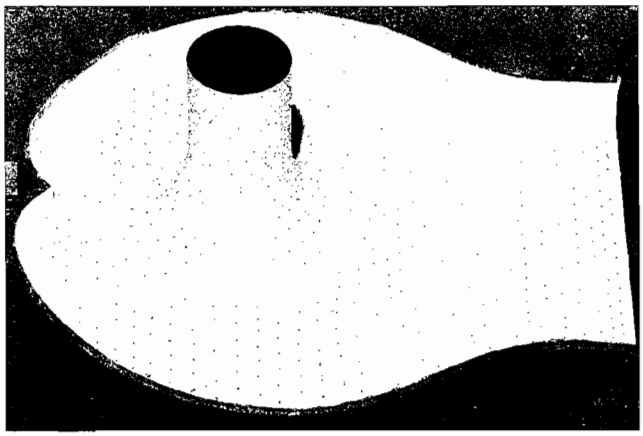

Figure 23. Wall Streamline Traces on Interior of Intake B-2. View of intake half-section opposite pump entry plane. Flow enters from the right.

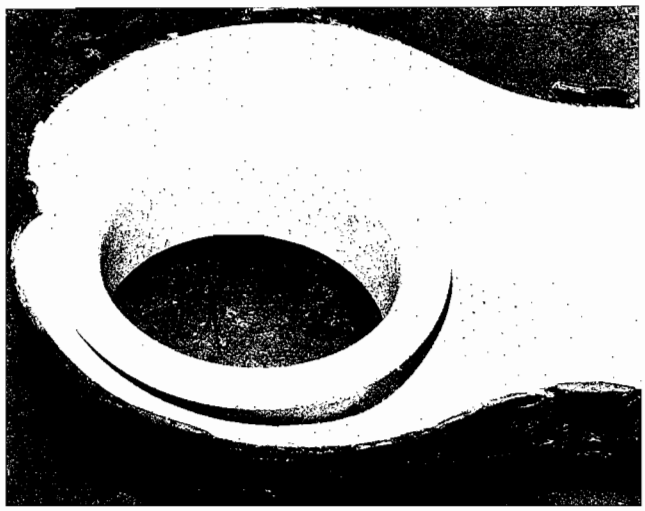

Figure 24. Wall Streamline Traces on Interior of Intake B-2. View of intake half-section including pump entry plane. Flow enters from the right.

horseshoe vortex formed at the intersection of the shaft with the flat doughnut wall. The importance of the horseshoe vortex effect is illustrated by a comparison of the twin vortex loss peaks in intakes A-1 and A-2. A thicker boundary layer would have entered the doughnut in the A-1 intake, due to the upstream diffusion, causing a stronger horseshoe vortex and the observed higher loss peaks. When the blade was moved to $\theta = 30°$ or $-30°$ (330°), the loss peaks shifted accordingly. Filling the doughnut cavity (Figure 2) increased the loss dramatically and spread it over a larger region. The introduction of posts had a mixed effect. The rectangular post at $\theta = 180°$ increased the loss in that region. The posts at 90° and 270° had a beneficial effect in that they dissipated the loss peaks at the pump entry associated with the twin vortices, although the wall streamline traces show the losses essentially unchanged on the flat face of the doughnut. The most dramatic effect of the posts was when they were included with a filled doughnut. In that case, the extra loss due to the filled doughnut disappeared in the presence of the posts.

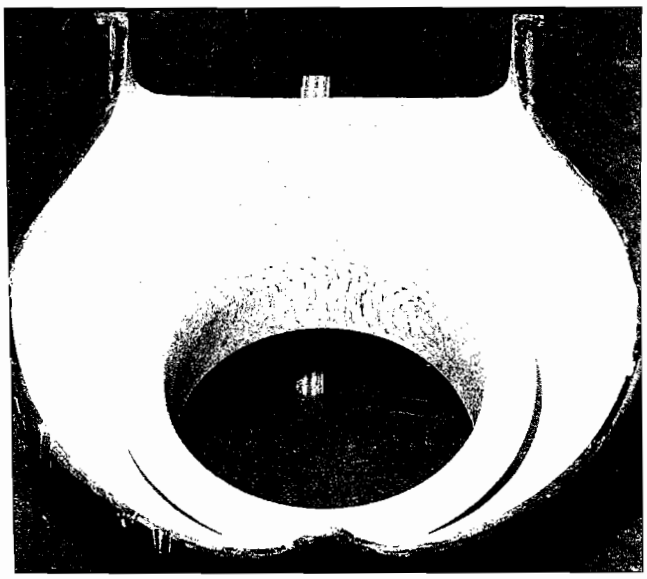

Figure 25. Wall Streamline Traces on Interior of Intake B-2. View of intake half-section including pump entry plane. Flow enters from top.

CONCLUSIONS

An air flow model has been used to effectively and relatively rapidly compare the performances and internal flow fields for a series of right angle minimum axial depth pump intakes. The test series included intakes with decelerating flow, usually avoided in intake design and, thus, rarely studied. A wall streamline flow visualization method has been extended to allow its application to curved surfaces.

It has been proven possible to produce acceptable intakes incorporating a decelerating flow and a restricted axial depth. Where design requirements allow, the diffusion within the intake should be minimized or indeed replaced with accelerating flow. The performance of diffusing intakes has been shown to be very sensitive to both the location of the flow diffusion and to the detailed internal shape of the intake. The evidence from the series A intakes is that although a diffusing doughnut is inferior to one with accelerating flow, diffusion immediately upstream of the doughnut seriously distorts the flow through the intake. It should also be noted that the complex design of the B-1 intake, which had upstream diffusion followed by an accelerating bend, had a higher average loss coefficient than the A-2 intake with the same overall area ratio but with all the diffusion in the doughnut. Nevertheless, since the observed flow distribution at the pump inlet plane was decidedly smoother for the B-1 intake, it is expected that a pump with a B-1 intake geometry would have superior performance to one with an A-2 intake.

Two major loss locations were observed and flow angle observations and wall streamline flow visualization assisted in establishing the flow pattern in these regions. The first was flow separation as the flow turned from the radial to the axial direction at the entry side of the doughnut. It is suggested that local wall curvature and increased axial depth should relieve this problem. However, the evidence from the B series intakes is that complex flow fields in this region can produce high losses even with modest curvature. The second loss region is characterized by twin vortices on the side of the doughnut opposite the flow entry. The flow field here is strongly influenced by the interrelation between the shaft, the intake surface opposite the pump entry plane, and the intake shape in the region of the blade. Small changes in the geometry can have major effects. Also, the twin vortex pattern is strongly affected by the flow condition entering the doughnut. The geometric shape of the B series intakes avoids the formation of the twin vortex pattern.

REFERENCES

1. Kovats, A., "Effect of Non-Rotating Passages on Performance of Centrifugal Pumps and Subsonic Compressors," *Flow in Primary Non-Rotating Passages in Turbomachines,* ASME, pp. 1-14 (December 1979).
2. Pilarczyk, K. and Rusak, V., "Application of Air Model Testing in the Study of Inlet Flow in Pumps," *Cavitation in Fluid Machinery,* ASME, pp. 91-108 (November 1965).
3. Bernard, T., "Inlet Boxes of Axial Fans," Proceedings of Third Conference on Fluid Mechanics and Fluid Machines, Budapest, pp. 37-43 (1969).
4. ASHRAE, *Handbook of Fundamentals,* Chap. 33, ASHRAE, Atlanta (1981).
5. Langston, L. S. and Boyle, M. T., "A New Surface Streamline Flow Visualization Technique," Journal of Fluid Mechanics, *125,* pp. 53-57 (December 1982).

ACKNOWLEDGEMENT

The experimental program described here was carried out at the University of Waterloo under a contract, through the Waterloo Research Institute, with Sundstrand Corporation, whose permission to publish this report is gratefully acknowledged by the authors. The construction, tests and data organization were carried out by C. Hadfield, G. Duncan, S. Coutts, P. Greene, C. K. Min, M. Holierhoek and O. Mukker.